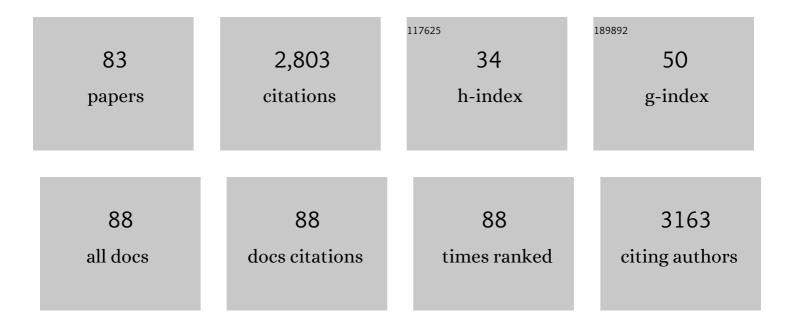
## **Gregory Holland**

List of Publications by Year in descending order

Source: https://exaly.com/author-pdf/8646942/publications.pdf

Version: 2024-02-01



#	Article	IF	CITATIONS
1	Assembly and Thermal-Induced Polymerization of Histidine on Fumed Silica Surfaces. ACS Earth and Space Chemistry, 2022, 6, 1552-1562.	2.7	0
2	Aciniform Spider Silk: Hydrationâ€Induced βâ€Sheet Crosslinking of αâ€Helicalâ€Rich Spider Preyâ€Wrapping S (Adv. Funct. Mater. 13/2021). Advanced Functional Materials, 2021, 31, 2170090.	ilk 14.9	0
3	Investigating the Atomic and Mesoscale Interactions that Facilitate Spider Silk Protein Pre-Assembly. Biomacromolecules, 2021, 22, 3377-3385.	5.4	6
4	The impact of metal doping on fumed silica structure and amino acid thermal condensation catalytic properties. Journal of Materials Science, 2021, 56, 16916-16927.	3.7	1
5	Hydrationâ€Induced βâ€5heet Crosslinking of αâ€Helicalâ€Rich Spider Preyâ€Wrapping Silk. Advanced Functior Materials, 2021, 31, 2007161.	nal 14.9	14
6	Selective One-Dimensional <sup>13</sup> C– <sup>13</sup> C Spin-Diffusion Solid-State Nuclear Magnetic Resonance Methods to Probe Spatial Arrangements in Biopolymers Including Plant Cell Walls, Peptides, and Spider Silk. Journal of Physical Chemistry B, 2020, 124, 9870-9883.	2.6	11
7	Probing the binding modes and dynamics of histidine on fumed silica surfaces by solid-state NMR. Physical Chemistry Chemical Physics, 2020, 22, 20349-20361.	2.8	12
8	Experimental Methods for Characterizing the Secondary Structure and Thermal Properties of Silk Proteins. Macromolecular Rapid Communications, 2019, 40, e1800390.	3.9	55
9	Investigating the interaction of Grammostola rosea venom peptides and model lipid bilayers with solid-state NMR and electron microscopy techniques. Biochimica Et Biophysica Acta - Biomembranes, 2019, 1861, 151-160.	2.6	3
10	Hierarchical Spidroin Micellar Nanoparticles as the Precursors of Spider Silks. Microscopy and Microanalysis, 2019, 25, 1346-1347.	0.4	0
11	Entropic effects enable life at extreme temperatures. Science Advances, 2019, 5, eaaw4783.	10.3	7
12	2H NMR reveals liquid state-like dynamics of arene guests inside hexameric pyrogallol[4]arene capsules in the solid state. Organic Chemistry Frontiers, 2019, 6, 1361-1366.	4.5	1
13	Fusion of Bipolar Tetraether Lipid Membranes Without Enhanced Leakage of Small Molecules. Scientific Reports, 2019, 9, 19359.	3.3	3
14	Hierarchical spidroin micellar nanoparticles as the fundamental precursors of spider silks. Proceedings of the National Academy of Sciences of the United States of America, 2018, 115, 11507-11512.	7.1	46
15	Spider prey-wrapping silk is an α-helical coiled-coil/β-sheet hybrid nanofiber. Chemical Communications, 2018, 54, 10746-10749.	4.1	13
16	Hybrid Lipids Inspired by Extremophiles and Eukaryotes Afford Serumâ€6table Membranes with Low Leakage. Chemistry - A European Journal, 2017, 23, 6757-6762.	3.3	12
17	Mechanically induced pyrogallol[4]arene hexamer assembly in the solid state extends the scope of molecular encapsulation. Chemical Science, 2017, 8, 7737-7745.	7.4	17
18	Thiol-Triggered Release of Intraliposomal Content from Liposomes Made of Extremophile-Inspired Tetraether Lipids. Bioconjugate Chemistry, 2017, 28, 2041-2045.	3.6	11

#	Article	IF	CITATIONS
19	Highly Efficient Fumed Silica Nanoparticles for Peptide Bond Formation: Converting Alanine to Alanine Anhydride. ACS Applied Materials & Interfaces, 2017, 9, 17653-17661.	8.0	28
20	Secondary Structure Adopted by the Gly-Gly-X Repetitive Regions of Dragline Spider Silk. International Journal of Molecular Sciences, 2016, 17, 2023.	4.1	29
21	Cyclohexane Rings Reduce Membrane Permeability to Small Ions in Archaeaâ€Inspired Tetraether Lipids. Angewandte Chemie, 2016, 128, 1922-1925.	2.0	5
22	Cyclohexane Rings Reduce Membrane Permeability to Small Ions in Archaeaâ€Inspired Tetraether Lipids. Angewandte Chemie - International Edition, 2016, 55, 1890-1893.	13.8	31
23	Effect of Headgroups on Smallâ€ion Permeability across Archaeaâ€inspired Tetraether Lipid Membranes. Chemistry - A European Journal, 2016, 22, 8074-8077.	3.3	15
24	Lysine-Capped Silica Nanoparticles: A Solid-State NMR Spectroscopy Study. MRS Advances, 2016, 1, 2261-2266.	0.9	7
25	Direct Evidence of Chelated Geometry of Catechol on TiO <sub>2</sub> by a Combined Solid-State NMR and DFT Study. Journal of Physical Chemistry C, 2016, 120, 23625-23630.	3.1	55
26	Thermal and Structural Properties of Silk Biomaterials Plasticized by Glycerol. Biomacromolecules, 2016, 17, 3911-3921.	5.4	40
27	Structure and Properties in Synthetic MSUM and the Corresponding Biomaterial. MRS Advances, 2016, 1, 2551-2556.	0.9	1
28	Solid-State NMR Characterization of Mixed Phosphonic Acid Ligand Binding and Organization on Silica Nanoparticles. Langmuir, 2016, 32, 3253-3261.	3.5	43
29	Molecular Dynamics of Spider Dragline Silk Fiber Investigated by <sup>2</sup> H MAS NMR. Biomacromolecules, 2015, 16, 852-859.	5.4	23
30	Probing the Impact of Acidification on Spider Silk Assembly Kinetics. Biomacromolecules, 2015, 16, 2072-2079.	5.4	15
31	Extended Charge Carrier Lifetimes in Hierarchical Donor–Acceptor Supramolecular Polymer Films. Journal of Physical Chemistry C, 2015, 119, 19584-19589.	3.1	25
32	Alanine Adsorption and Thermal Condensation at the Interface of Fumed Silica Nanoparticles: A Solid-State NMR Investigation. Journal of Physical Chemistry C, 2015, 119, 25663-25672.	3.1	37
33	Are Spider Silk Proteins a New Class of Intrinsically Disordered Proteins?. Biophysical Journal, 2014, 106, 686a.	0.5	0
34	Investigating Lysine Adsorption on Fumed Silica Nanoparticles. Journal of Physical Chemistry C, 2014, 118, 25792-25801.	3.1	52
35	Elucidating proline dynamics in spider dragline silk fibre using <sup>2</sup> H– <sup>13</sup> C HETCOR MAS NMR. Chemical Communications, 2014, 50, 4856-4859.	4.1	20
36	Structural characterization of nanofiber silk produced by embiopterans (webspinners). RSC Advances, 2014, 4, 41301-41313.	3.6	20

#	Article	IF	CITATIONS
37	Probing the Nature of Charge Transfer at Nano–Bio Interfaces: Peptides on Metal Oxide Nanoparticles. Journal of Physical Chemistry Letters, 2014, 5, 3555-3559.	4.6	11
38	Reversible Assembly of β-Sheet Nanocrystals within Caddisfly Silk. Biomacromolecules, 2014, 15, 1269-1275.	5.4	34
39	Exploring the backbone dynamics of native spider silk proteins in Black Widow silk glands with solution-state NMR spectroscopy. Polymer, 2014, 55, 3879-3885.	3.8	23
40	NMR Characterization of Spider Venom Neurotoxin Structure and Interactions with Lipid Bilayers. Biophysical Journal, 2014, 106, 294a.	0.5	0
41	Structural Characterization of Caddisfly Silk with Solid-State NMR and X-Ray Diffraction. Biophysical Journal, 2014, 106, 227a.	0.5	1
42	Probing site-specific 13C/15N-isotope enrichment of spider silk with liquid-state NMR spectroscopy. Analytical and Bioanalytical Chemistry, 2013, 405, 3997-4008.	3.7	8
43	Silk structure studied with nuclear magnetic resonance. Progress in Nuclear Magnetic Resonance Spectroscopy, 2013, 69, 23-68.	7.5	88
44	Amino acid analysis of spider dragline silk using 1H NMR. Analytical Biochemistry, 2013, 440, 150-157.	2.4	9
45	Characterizing the Secondary Protein Structure of Black Widow Dragline Silk Using Solid-State NMR and X-ray Diffraction. Biomacromolecules, 2013, 14, 3472-3483.	5.4	69
46	Elucidating silk structure using solid-state NMR. Soft Matter, 2013, 9, 11440.	2.7	65
47	Determining hydrogen-bond interactions in spider silk with 1H–13C HETCOR fast MAS solid-state NMR and DFT proton chemical shift calculations. Chemical Communications, 2013, 49, 6680.	4.1	15
48	β-Sheet Nanocrystalline Domains Formed from Phosphorylated Serine-Rich Motifs in Caddisfly Larval Silk: A Solid State NMR and XRD Study. Biomacromolecules, 2013, 14, 1140-1148.	5.4	69
49	Probing lipid–cholesterol interactions in DOPC/eSM/Chol and DOPC/DPPC/Chol model lipid rafts with DSC and 13C solid-state NMR. Biochimica Et Biophysica Acta - Biomembranes, 2013, 1828, 1889-1898.	2.6	52
50	2H–13C HETCOR MAS NMR for indirect detection of 2H quadrupole patterns and spin–lattice relaxation rates. Journal of Magnetic Resonance, 2013, 226, 1-12.	2.1	14
51	Processing of meteoritic organic materials as a possible analog of early molecular evolution in planetary environments. Proceedings of the National Academy of Sciences of the United States of America, 2013, 110, 15614-15619.	7.1	34
52	Reproducing Natural Spider Silks' Copolymer Behavior in Synthetic Silk Mimics. Biomacromolecules, 2012, 13, 3938-3948.	5.4	46
53	High resolution magic angle spinning NMR investigation of silk protein structure within major ampullate glands of orb weaving spiders. Soft Matter, 2012, 8, 1947-1954.	2.7	37
54	Investigating Hydrogen-Bonded Phosphonic Acids with Proton Ultrafast MAS NMR and DFT Calculations. Journal of Physical Chemistry C, 2012, 116, 18824-18830.	3.1	16

#	Article	IF	CITATIONS
55	Combining flagelliform and dragline spider silk motifs to produce tunable synthetic biopolymer fibers. Biopolymers, 2012, 97, 418-431.	2.4	67
56	Inducing β-Sheets Formation in Synthetic Spider Silk Fibers by Aqueous Post-Spin Stretching. Biomacromolecules, 2011, 12, 2375-2381.	5.4	69
57	NMR Determination of the Diffusion Mechanisms in Triethylamine-Based Protic Ionic Liquids. Journal of Physical Chemistry Letters, 2011, 2, 1077-1081.	4.6	43
58	Abundant ammonia in primitive asteroids and the case for a possible exobiology. Proceedings of the National Academy of Sciences of the United States of America, 2011, 108, 4303-4306.	7.1	85
59	Ultrahydrous stishovite from high-pressure hydrothermal treatment of SiO <sub>2</sub> . Proceedings of the National Academy of Sciences of the United States of America, 2011, 108, 20918-20922.	7.1	36
60	Proton-detected heteronuclear single quantum correlation NMR spectroscopy in rigid solids with ultra-fast MAS. Journal of Magnetic Resonance, 2010, 202, 64-71.	2.1	44
61	Quantitative Correlation between the Protein Primary Sequences and Secondary Structures in Spider Dragline Silks. Biomacromolecules, 2010, 11, 192-200.	5.4	107
62	Structure and Dynamics of Aromatic Residues in Spider Silk: 2D Carbon Correlation NMR of Dragline Fibers. Biomacromolecules, 2010, 11, 168-174.	5.4	36
63	Solid-State NMR Comparison of Various Spiders' Dragline Silk Fiber. Biomacromolecules, 2010, 11, 2039-2043.	5.4	65
64	Solid-state NMR evidence for elastin-like β-turn structure in spider dragline silk. Chemical Communications, 2010, 46, 6714.	4.1	95
65	Vibrational properties of the gallium monohydrides SrGaGeH, BaGaSiH, BaGaGeH, and BaGaSnH. Journal of Solid State Chemistry, 2009, 182, 2068-2073.	2.9	14
66	Structural and Dynamic Properties of BalnGeH: A Rare Solid-State Indium Hydride. Inorganic Chemistry, 2009, 48, 5602-5604.	4.0	13
67	NMR Characterization of Ligand Binding and Exchange Dynamics in Triphenylphosphine-Capped Gold Nanoparticles. Journal of Physical Chemistry C, 2009, 113, 16387-16393.	3.1	65
68	Unique Backbone-Water Interaction Detected in Sphingomyelin Bilayers with 1H/31P and 1H/13C HETCOR MAS NMR Spectroscopy. Biophysical Journal, 2008, 95, 1189-1198.	0.5	12
69	Quantifying the fraction of glycine and alanine in β-sheet and helical conformations in spider dragline silk using solid-state NMR. Chemical Communications, 2008, , 5568.	4.1	70
70	Solid-State NMR Investigation of Major and Minor Ampullate Spider Silk in the Native and Hydrated States. Biomacromolecules, 2008, 9, 651-657.	5.4	92
71	Polyanionic Gallium Hydrides from AlB2-Type Precursors AeGaE (Ae = Ca, Sr, Ba; E = Si, Ge, Sn). Journal of the American Chemical Society, 2008, 130, 12139-12147.	13.7	36
72	Determining Secondary Structure in Spider Dragline Silk by Carbonâ^'Carbon Correlation Solid-State NMR Spectroscopy. Journal of the American Chemical Society, 2008, 130, 9871-9877.	13.7	147

#	Article	IF	CITATIONS
73	NMR Characterization of Phosphonic Acid Capped SnO2Nanoparticles. Chemistry of Materials, 2007, 19, 2519-2526.	6.7	92
74	Distinguishing Individual Lipid Headgroup Mobility and Phase Transitions in Raft-Forming Lipid Mixtures with 31P MAS NMR. Biophysical Journal, 2006, 90, 4248-4260.	0.5	47
75	Solid-State Structural Characterization of a Rigid Framework of Lacunary Heteropolyniobates. Inorganic Chemistry, 2006, 45, 1043-1052.	4.0	92
76	Magnetic alignment of aqueous CTAB in nematic and hexagonal liquid crystalline phases investigated by spin-1 NMR. Physical Chemistry Chemical Physics, 2006, 8, 2635.	2.8	29
77	1H–13C INEPT MAS NMR correlation experiments with 1H–1H mediated magnetization exchange to probe organization in lipid biomembranes. Journal of Magnetic Resonance, 2006, 180, 210-221.	2.1	14
78	Multi-dimensional 1H–13C HETCOR and FSLG-HETCOR NMR study of sphingomyelin bilayers containing cholesterol in the gel and liquid crystalline states. Journal of Magnetic Resonance, 2006, 181, 316-326.	2.1	28
79	Location and Orientation of Adsorbed Molecules in Zeolites from Solid-State REAPDOR NMR. ChemInform, 2005, 36, no.	0.0	0
80	Location and orientation of adsorbed molecules in zeolites from solid-state REAPDOR NMR. Physical Chemistry Chemical Physics, 2005, 7, 1739.	2.8	20
81	Distribution effects on 1H double-quantum MAS NMR spectra. Journal of Magnetic Resonance, 2004, 167, 161-167.	2.1	17
82	WISE NMR Characterization of Nanoscale Heterogeneity and Mobility in SupercontractedNephila clavipesSpider Dragline Silk. Journal of the American Chemical Society, 2004, 126, 5867-5872.	13.7	104
83	7Li NMR Studies of Electrochemically Lithiated V2O5Xerogels. Chemistry of Materials, 2002, 14,	6.7	15